Heliyon 7 (2021) e06963

Contents lists available at ScienceDirect

Heliyon

journal homepage: www.cell.com/heliyon

Research article

Enhanced multi functionality of semi-refined iota carrageenan as food packaging material by incorporating SiO_2 and ZnO nanoparticles

Danar Praseptiangga [a,*], Nuha Mufida [a,c], Camellia Panatarani [b,c], I.Made Joni [b,c]

[a] Department of Food Science and Technology, Faculty of Agriculture, Universitas Sebelas Maret (UNS), Jl Ir. Sutami 36 A, Kentingan, Jebres, 57126, Surakarta, Central Java, Indonesia
[b] Department of Physics, Faculty of Mathematics and Natural Sciences, Universitas Padjadjaran, Jl Raya Bandung-Sumedang KM 21, Jatinangor, West Java, 45363, Indonesia
[c] Functional Nano Powder University Center of Excellence, Universitas Padjadjaran, Jl Raya Bandung-Sumedang KM 21, Jatinangor, West Java, 45363, Indonesia

ARTICLE INFO

Keywords:
Iota carrageenan
Nanoparticles
Nanocomposite film
Food packaging

ABSTRACT

This paper reports the incorporation of SiO_2–ZnO nanoparticles (NPs) into semi-refined iota carrageenan-based (SRIC) film as active food packaging. The dispersion of the nanoparticles was performed using a bead milling method and the films were prepared using the solution casting method. The incorporation of SiO_2–ZnO NPs into SRIC films aims to provide multifunctional food packaging with enhanced water vapor barrier properties, UV-screening, and antimicrobial activity. The effect of the incorporation of SiO_2 NPs, ZnO NPs, and the mixtures of SiO_2–ZnO NPs varied in SiO_2/ZnO ratios (SiO_2–ZnO 1:1, 1:2, and 1:3) were investigated. The results showed that the tensile strength, water vapor barrier performance, UV-screening, and antimicrobial activity of the SRIC film were increased by the addition of either SiO_2 or ZnO NPs alone. Interestingly, when the mixtures of SiO_2–ZnO were incorporated, more significant improvement was observed. Also, the bio-degradability and solubility of all the SRIC films were confirmed. It was concluded that the SiO_2–ZnO NPs incorporated into SRIC film provided multifunctional activities and acted as a promising active food packaging material.

1. Introduction

Since food packaging made of non-renewable petrochemical materials has been found to cause health and environmental issues, the application of biopolymers as food packaging materials has increased, due to their degradability, availability, relatively low cost, biocompatibility, and nontoxicity [1, 2, 3]. The most common types of biopolymers as the main biodegradable films material are polysaccharides, proteins, and lipids [4, 5]. Polysaccharides are abundantly available and interesting biopolymers due to their superior film-forming ability, good colloidal nature, acceptable gas barrier, and strong mechanical characteristics [3, 6]. Iota carrageenan is one of the polysaccharide-types containing sulfate groups extracted from red algae (*Eucheuma denticulatum*) which can be used as a material to form film matrices. Besides its abundant availability and suboptimal utilization, the properties of iota carrageenan are very suitable to be applied as film-forming material [7, 8]. Iota carrageenan-based films exhibit several advantages, such as good mechanical properties, emulsion stability, and oxygen barrier [9, 10].

However, biopolymers exhibit several weaknesses when applied as food packaging materials, including relatively low mechanical and water barrier properties. To overcome these weaknesses and improve the film properties including providing UV blocking and antimicrobial features while maintaining the biodegradable characteristic, nanoparticles have been widely incorporated into the various biopolymer-based films, forming a bio-nanocomposite film [1, 11]. Bio-nanocomposite is a multiphase material composed of two or more elements with a biopolymer as a continuous phase or matrix and nanofiller as a discontinuous phase [2]. The large surface to volume ratio of nanoparticles leads to form more interactions with the polymer matrix thus increasing their effect on improving film properties [12]. Furthermore, blending organic and inorganic materials to form composite materials may bring more advantages which come from both the organic and inorganic materials [13].

Different types of nanoparticles have been incorporated into biopolymer-based films to improve their characteristics, including silicon dioxide, zinc oxide, titanium dioxide, copper, silver, and gold nanoparticles, which provide excellent features such as antimicrobial activity,

* Corresponding author.
E-mail address: dpraseptiangga@staff.uns.ac.id (D. Praseptiangga).

https://doi.org/10.1016/j.heliyon.2021.e06963
Received 16 January 2021; Received in revised form 22 March 2021; Accepted 26 April 2021

water vapor and oxygen barrier enhancement, and UV protection [14, 15, 16, 17]. The advantages of silicon dioxide (SiO_2) nanoparticles compared to other particles are stable, non-toxic, and safe food additives used in food processing and preservation [15]. While zinc oxide (ZnO) nanoparticles demonstrate the strongest antimicrobial activity against numerous microorganisms, are more affordable, and listed as generally recognized as safe (GRAS) material compared to other metal oxide nanoparticles [16, 18]. Moreover, ZnO nanoparticles have been widely applied as nanofillers in improving the packaging properties due to their crystalline structure, high stability, excellent mechanical properties, strong antibacterial activity, and high UV absorption capacity [13, 19].

Independent application of either SiO_2 or ZnO nanoparticles (NPs) as fillers in the carrageenan-based film has been reported in improving the film properties in previous studies [1, 20, 21, 22, 23]. Among them, the utilization of semi-refined carrageenan to produce bio-nanocomposite film is more interesting with considerably low production cost compare to the refined form which is relatively expensive. Moreover, there were only limited studies on developing bio-nanocomposite film with the semi-refined iota carrageenan (SRIC) as the main film matrix. Previous studies showed the incorporation of SiO_2 NPs and ZnO NPs separately enhanced the properties of SRIC films [1, 21]. Also, recent study showed that SiO_2 NPs as fillers provided antimicrobial functionality [24]. These various advantages raised the question of whether the incorporation of the mixture of SiO_2 NPs and ZnO NPs into SRIC film could provide enhanced multi-functionalities of film such as UV blocking, antimicrobial, and water barrier as required in active food packaging applications better than when these nanoparticles were used separately.

Although the incorporation of nanoparticles into biopolymer film had been reported in many studies, these studies did not focus on the method to incorporate the nanoparticle into the film. Nanoparticles are easily agglomerated when dispersed in an aqueous phase [25], while a well-dispersed nanoparticles suspension is required to be achieved in the making of bio-nanocomposite film since the bad dispersion of nanoparticles and the formed-agglomerates in the suspension could diminish their performances to produce more desirable film properties [12]. As reported in previous researches, bead milling is the preferable method to disperse nanoparticles in suspension [24, 25, 26, 27, 28]. In the bead milling method, the collisions between micro-sized beads and the nanoparticles by continuous agitation result in well-dispersed and stable suspension [29]. No other studies used this method to prepare bio-nanocomposite film before. Meanwhile, preliminary studies have revealed the effectiveness of the bead milling in dispersing SiO_2–ZnO NPs and breaking up the agglomerates in suspension [29]. Furthermore, the FTIR spectra observation of dispersed SiO_2–ZnO NPs mixture after bead milling showed prospective surface functional groups [30].

The novelty of this present study is the incorporation of SiO_2–ZnO NPs combinations prepared by bead milling process into semi-refined iota carrageenan-based (SRIC) film as active food packaging provided enhanced water vapor barrier, UV-screening, and antimicrobial activity. Despite the active functionality of the SRIC film, other determining characteristics and related properties of the film were also observed such as surface morphology, mechanical properties, transparency, wettability, water-solubility, degradability, and thermal stability.

2. Materials and methods

2.1. Materials

Semi-refined iota carrageenan (SRIC) powder was purchased from Galic Artabahari, Co., Ltd. (Bekasi, Indonesia). Glycerol and Sodium dodecyl sulfate (SDS) were purchased from Brataco, Co., Ltd. (Bandung, Indonesia). SiO_2 NPs powder and ZnO NPs powder with a particle size of ±50 nm and 100–200 nm respectively were received from JP Cipta Nanotech Indonesia Ltd. (Bandung, Indonesia). *Escherichia coli* and *Staphylococcus aureus* were obtained from the Department of Biology, Universitas Padjadjaran (Bandung, Indonesia).

2.2. Preparation of bio-nanocomposite film

Before being added to the film solutions, the nanoparticles need to be dispersed into the water first to form NPs suspensions. In this study, five different NPs formulas were used: SiO_2 (0.5%), ZnO (1%), SiO_2–ZnO 1:1 (0.5%:0.5%), SiO_2–ZnO 1:2 (0.5%:1%), and SiO_2–ZnO 1:3 (0.5%:1.5%), based on the percentage of nanoparticle weight to carrageenan weight (% w/w carrageenan). The NPs suspensions were produced using the bead milling process in order to generate a good dispersion of nanoparticles, as reported in a previous study [29]. 150 g of suspension containing nanoparticles, SDS surfactant, and distilled water was prepared for bead milling process. The NPs powder according to each NPs formula was dispersed into distilled water and stirred for an hour, followed by adding the SDS surfactant (10 % w/w NPs) and stirred again for 1 h. After being sonicated for 30 min, the suspension was bead milled for 2 h. In the bead milling process, the suspension was agitated in the vessel containing 150 mL of zirconia beads using an agitator which the speed was set up at 30 Hz. The vessel was coated with a cooling water jacket to prevent temperature rise in system. A detailed description of the bead mill has been reported in previous studies [24, 25, 27].

Based on the NPs formulas, six different film types were produced: IC (SRIC film without nanoparticles), IC/SiO_2 (SRIC film incorporated with SiO_2), IC/ZnO (SRIC film incorporated with ZnO), IC/SiO_2–ZnO 1:1 (SRIC film incorporated with SiO_2–ZnO 1:1), IC/SiO_2–ZnO 1:2 (SRIC film incorporated with SiO_2–ZnO 1:2), and IC/SiO_2–ZnO 1:3 (SRIC film incorporated with SiO_2–ZnO 1:3). The concentration of SiO_2 remained the same in all the formulas, referring to Aji et al. [21] and Rane et al. [23], which found that the concentration of SiO_2 nanoparticles that imparts the best film properties was 0.5% w/w carrageenan. Whereas the concentration of ZnO nanoparticles was increased, referring to Oun & Rhim [31] and Khoirunnisa et al. [1], which demonstrated that the film properties increased as the ZnO concentration was increased.

The bio-nanocomposite films were prepared using the solution casting method, referring to Khoirunnisa et al. [1] with modifications. 100 g of the film solution was prepared, firstly by added 15 g of bead milled NPs suspension into distilled water and sonicated (30 min), then 2 g of SRIC powder was added. Subsequently, the film solution was heated to 70 °C, then glycerol (1 % w/w film solution) was added while stirring continuously for 10 min at 70 °C. Once the temperature had decreased to 50 °C, the film solution was poured onto a plastic plate (24 × 16 cm) and waited until turn to gel before drying it in the oven (50 °C; 3 h). Then the dried film was peeled off from the plate and stored in a relatively low RH cabinet for further characterizations. The other types of film were produced in the same way, except for the IC film which was produced by adding SRIC powder into distilled water without nanoparticles.

2.3. Film characterizations

2.3.1. Surface morphology

Scanning Electron Microscopy (SEM) and Atomic Force Microscopy (AFM) were used to observe the surface morphology and characteristic of the films [32]. For the SEM analysis procedure, the film samples were coated with gold to improve contrast and the signal-to-noise ratio as the samples were categorized as non-conductive samples.

2.3.2. Fourier transform infrared (FTIR)

FTIR spectrometer was used to analyze the functional groups of the constituent materials and film samples. The infra-red (IR) spectrum was measured at a range of 4000–400 cm^{-1} wavenumber at room temperature [33].

2.3.3. Thickness

The average thickness of the film was obtained by measuring at five different points using a Digital Micrometer (KRISBOW KW06-85) with 0.001 mm of accuracy [34].

2.3.4. Mechanical properties

The Tensile Strength (TS) and the Elongation at Break (EAB) were measured using a Universal Testing Machine with a test speed of 10 mm/min and operated under ASTM D 882-02 [35]. The TS and EAB were calculated as follows (Eqs. (1) and (2)):

$$\text{TS (MPa)} = \frac{\text{maximum load (N)}}{\text{initial cross} - \text{sectional area}(\text{m}^2)} \quad (1)$$

$$\text{EAB (\%)} = \frac{\text{elongated length at break}}{\text{initial length}} \times 100 \quad (2)$$

2.3.5. Water vapor permeability (WVP)

The WVP was determined gravimetrically according to the ASTM E96-00 with modifications [33, 36]. The test cup was filled with anhydrous $CaCl_2$ (3 g), then the film sample was placed over the top of the test cup and sealed with melted paraffin around the edges and placed in a humidity chamber (25 °C; 60% RH). The test cup was weighed every hour for 7 h. The weight changes were recorded as a function of time. The slope (g/h) was calculated from the linear regression. The WVP (10^{-6} g/h m Pa) was calculated using the following equation (Eq. (3)):

$$\text{WVP} = \frac{\text{WVTR x}}{\text{P}(\text{RH}_1 - \text{RH}_2)} \quad (3)$$

The water vapor transmission rate (WVTR) is the slope (g/h) divided by the transfer area (m^2), where x is the film sample thickness, P is the saturated water vapor pressure (at 25 °C), RH_1 is the RH inside the humidity chamber, and RH_2 is the RH inside the test cup.

2.3.6. Wettability

The wettability of the films was evaluated based on the critical surface tension (γ_c), which was determined by measuring the static contact angle of three different test liquids (deionized water, formamide, and n-hexadecane). The surface tension (γ) of each test liquid was entered as the *x*-axis, and the *cos* value from the contact angle (θ) measurement was entered as the *y*-axis in the linear regression analysis, for *cos* $\theta = 1$, because when *cos* $\theta = 1$, then $\gamma = \gamma_c$ [37].

2.3.7. Optical properties

The optical properties (transparency and UV-screening) were determined by measuring the transmittance (%) at the wavelength of 200–700 nm using a UV-Vis spectrophotometer. The film sample (3 × 1 cm) was placed on the cuvette wall which was illuminated by a UV-Vis light [38].

2.3.8. Antimicrobial activity

The antimicrobial activity was examined using the agar disc diffusion method [39], based on the inhibition against *Staphylococcus aureus* and *Escherichia coli*. The bacterial culture at a concentration of 1-2 x 10^8 CFU/ml (0.5 McFarland) was inoculated on the agar plate. Then the film sample (d = 7 mm) was put on the inoculated agar plate and incubated at 35 °C for 24 h. The diameter of the clear zone formed around the sample was measured as the inhibition zone.

2.3.9. Water-solubility

The film solubility in water was determined as described by Beigomi et al. [33] with modifications. The film sample (3 × 3 cm) was dried in an oven (100 °C; 6 h) and weighed to determine the dry basis. The sample was then immersed into distilled water (50 ml) under constant stirring for 12 h, filtered using filter paper, and dried (100 °C; 6 h) to determine the un-soluble part of the sample. The water-solubility of the sample was calculated using Eq. (4), where w_i is the initial dry basis of the sample and w_f is the weight of the un-soluble part of the sample.

$$\text{WS (\%)} = \frac{\text{w}_\text{i} - \text{w}_\text{f}}{\text{w}_\text{i}} \times 100 \quad (4)$$

2.3.10. Degradability

The degradability was determined by a soil burial test, according to Swain et al. [40], to evaluate the weight loss of the film samples over time. The samples (3 × 3 cm) were buried in a bucket filled with soil to a depth of 10 cm. The bucket was covered to maintain its moisture and placed in a laboratory (25 °C). The samples were weighed every 7 days for 28 days. The weight loss of the samples over time was used to indicate the degradation rate.

2.3.11. Thermal stability

A thermogravimetry analysis (TGA) was used to determine the thermal stability of the films, according to Rhim & Wang [41] with some modifications. The samples were heated starting from room temperature up to 500 °C with a heating rate of 10 °C/min in a nitrogen atmosphere (25 ml/min).

2.3.12. Statistical analysis

SPSS software was used to perform statistical analyses of the experimental data using one-way ANOVA with a significant difference at a 5% level of probability ($p < 0.05$). The analyses were continued to the Duncan multiple range test if there was a significant difference in the results.

3. Results and discussion

3.1. Surface morphology

The surface morphology of the SRIC-based films observed using SEM showed the details of the surface structure of the film samples such as smoothness and cracks and the distribution of the nanoparticles on the film matrix [22]. As shown in Figure 1(a), the surface of the film without nanoparticles (IC) appeared smooth with only a few cracks, whereas the films with nanoparticles showed a rougher and non-homogeneous surface. It is in agreement with other studies that the surface morphology of carrageenan film becomes rough after the addition of ZnO nanoparticles [31, 38]. However, the IC/SiO_2–ZnO 1:3 film looked smoother and wavy.

The surface morphology was also observed using AFM to visualize the surface of the films in a three-dimensional relief to provide information about the surface contour of the films [42]. The surface of the IC film looked uneven with large lumps and dents. The surface of the films with SiO_2 and ZnO nanoparticles separately appeared rougher because of the presence of the nanoparticles. However, the surface of the films with the addition of SiO_2–ZnO 1:1 and 1:3 nanoparticles looked smoother and more even which indicated better compatibility of the nanoparticles in the film matrix (Figure 1(b)).

3.2. Fourier transform infrared (FTIR)

The FTIR result of the constituent materials is presented in Figure 2(a), while the FTIR result of the bio-nanocomposite films is presented in Figure 2(b). The transmittance peak of hydroxyl group *v* (O − H) was appeared around the wavenumber of 3561–3607 cm^{-1} for the bio-nanocomposite films, while for the constituent materials it was at 3379-3468 cm^{-1}. The hydroxyl group in the films indicated the presence of hydrogen bonds from the materials and adsorbed water [32, 43]. The wavenumber indicating the appearance of *v* $(CH)_a$ (*asymmetric* CH *stretching*) group was shifted to a greater value for the bio-nanocomposite films compared to the iota carrageenan, glycerol, and SDS. The SiO_2 and ZnO nanoparticles did not show peak absorbance in this region because they did not contain carbonyl groups. However, the peak was shifted to a smaller wavenumber for the film with the addition of SiO_2 nanoparticles (IC/SiO_2 film) compared to the IC film. Meanwhile, the film with the addition of ZnO nanoparticles (IC/ZnO film) did not show such a shift in

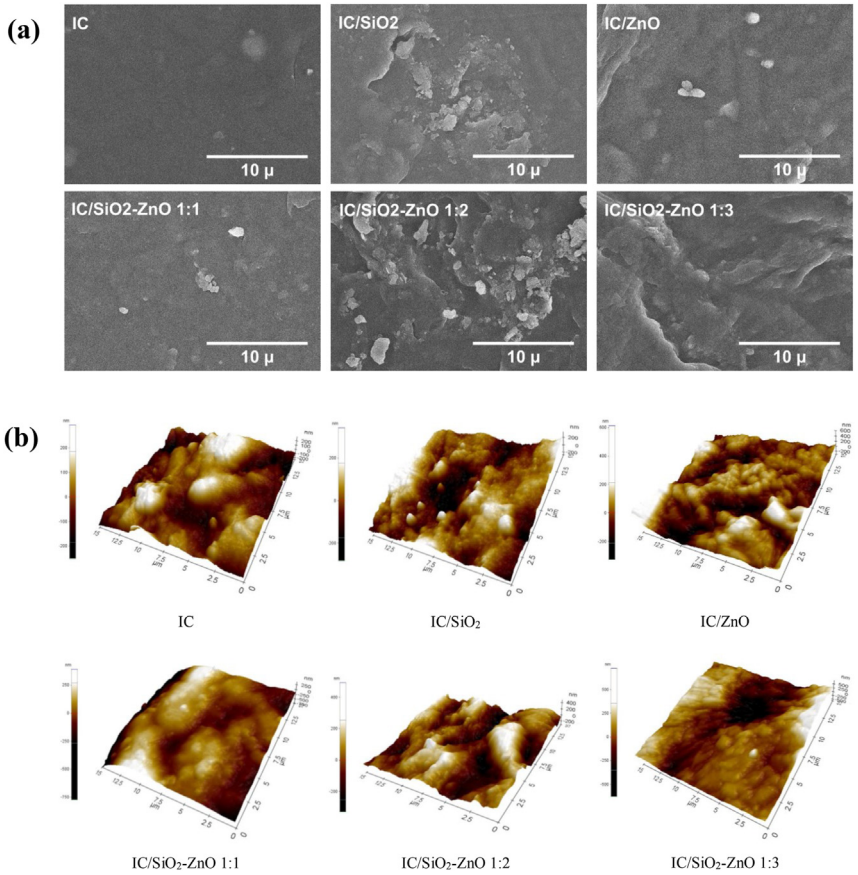

Figure 1. Surface morphology of the bio-nanocomposite films, (a) SEM images and (b) AFM images.

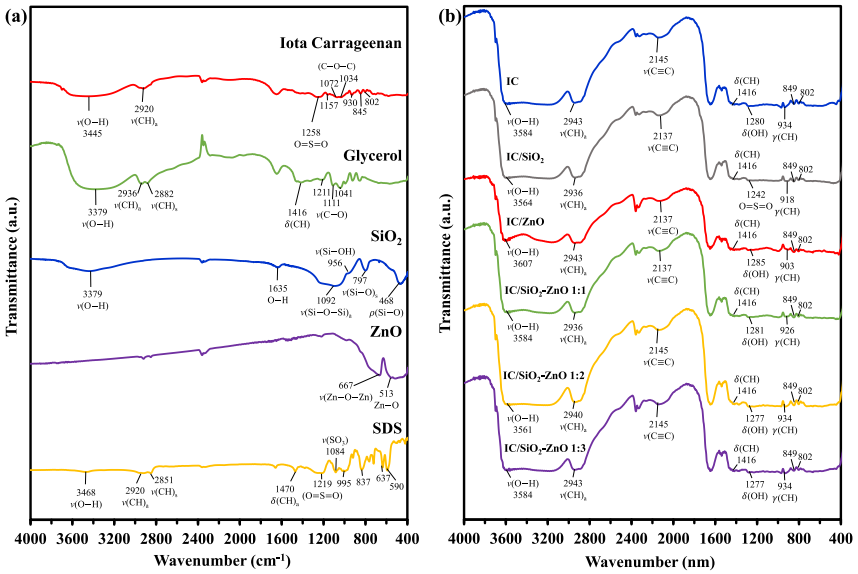

Figure 2. FTIR result of the (a) constituent materials and (b) bio-nanocomposite films. Notes: (v) stretching vibrations; (δ) bending vibrations (in the plane); (γ) bending vibrations (out of the plane); (ρ) rocking vibrations; ($_a$) coupled asymmetric; ($_s$) coupled symmetric.

the absorption peak. For the film with a combination of SiO_2 and ZnO (IC/SiO_2–ZnO 1:1), the wavenumber had a smaller value but shifted to a greater value along with the increment of ZnO concentration in the film.

The functional groups which were not found in the four constituent materials but were formed in all types of films were *v* (C≡ C) and γ(CH). The *δ*(OH) group was also not found in any of the constituent materials but appeared in all the film types except the IC/SiO_2 film. Contrarily, some functional groups were found in the constituent materials but did not appear in the films, i.e. the *v* (C − O) group in the glycerol, the $\delta(CH)_a$ group and sulfate group (*v* (SO_3)) in the SDS, and the C − O − C group and 3,6-anhydro-D-galactose group in the iota carrageenan. In addition, the groups found in either SiO_2 or ZnO were not detected in any types of film. The chemical interaction that occurred between the constituent materials may have led to a shift in the wavenumber for the resulting

films and changes in the film functional groups, therefore several functional groups were found in the constituent materials but did not appear in the films, and also there were new functional groups that appeared in the films but were not found in any of the constituent materials.

3.3. Thickness

The film thickness increased with the addition of SiO_2 and ZnO nanoparticles separately (Table 1), which is probably because the solid content in the film solution increased with the addition of nanoparticles. Other studies have reported a similar trend after the addition of ZnO NPs [38] and SiO_2 NPs into carrageenan-based films [34]. Whilst the thickness of the SiO_2–ZnO nanoparticles film was not significantly different from the IC film but significantly lower than the IC/SiO_2 and IC/ZnO films. The hydrogen atom from the hydroxyl group (O − H) in the film matrix interacted with the oxygen atom from the nanoparticle molecules to form a hydrogen bond. More hydrogen bonds were formed as the nanoparticle concentration was increased. This led to a reduction in the availability of the hydroxyl groups in the polymer to interact with H_2O molecules, thereby reducing the amount of water bounded in the film matrix so that the thickness was also reduced [44]. The decrease in thickness was also observed by another study which showed that the thickness of the starch/kefiran film decreased with increasing ZnO concentration. This phenomenon may occur under the influence of the type of polymer, the type of nanoparticles, the number of nanoparticles added, and the film preparation method [45].

3.4. Mechanical properties

The addition of either SiO_2 or ZnO nanoparticles caused an enhancement in the TS, but their combination caused the TS to decreased slightly, although not significantly (Table 1). However, as more ZnO nanoparticles were added, the TS also increased, although the standard deviations (SD) were quite larger in the IC/SiO_2–ZnO 1:2 and 1:3 films. A larger SD indicates a larger spread of the data distribution, which may be affected by the presence of outliers in the data. The increment in TS occurs due to the formation of strong hydrogen bonds between the nanoparticles and the hydroxyl groups in the film matrix [22] and the van der Waals force which strengthens the intermolecular forces between nanoparticles and carrageenan [21]. The IC/SiO_2–ZnO 1:3 film had the greatest TS. The TS values in this study were generally still much higher than in previous SRIC-based films such as SRIC/SiO_2 films (8.52–11.68 MPa) [21], and SRIC/palmitic acid films (4.621–6.268 MPa) [9]. The mechanical properties of films may also depend on the nanoparticle dispersion in the matrix polymers [12]. The SEM and AFM analysis show that the IC/SiO_2–ZnO 1:3 film had good nanoparticle dispersion and compatibility in the film matrix, which indicates a strong adhesion force, so it had the highest TS.

Generally, the EAB of all the films did not differ significantly (Table 1), which means there was no significant influence by the incorporation of nanoparticles into the film on its elongation. However, the standard deviations (SD) were also quite larger in the IC/SiO_2–ZnO 1:2 and 1:3 films. Nanoparticles are like ball bearings which make the movement of the polymer chain easier [46] and do not interfere with the movement of the polymer chain thereby the presence of nanoparticles can maintain or even increase the film elongation [38].

3.5. Water vapor permeability (WVP)

The WVP decreased as more nanoparticles were added (Table 1). This indicates that the SiO_2 and ZnO nanoparticles enhanced the moisture barrier properties of SRIC film. The formation of tortuous pathways in the polymer matrix by the presence of nanoparticles slows down the diffusion rate of water molecules to pass through the film, thus increasing the water vapor barrier [1, 44, 46].

The films with the combination of SiO_2–ZnO nanoparticles showed a lower WVP value compared to the films with only one type of nanoparticles. The interaction between the two types of nanoparticles may create a synergistic effect in improving the barrier properties against water vapor. Moreover, both types of nanoparticles are hydrophobic, thus would reduce the hydrophilicity of the SRIC film, and reducing the WVP [22, 34].

The rigidity of film structures might also have the effect on reducing the WVP. The nanoparticles fill the pores or empty spaces in macromolecular structures that are usually occupied by water molecules, leading to structural rigidity [44] which decreases the diffusion of water vapor molecules. Also, the formation of hydrogen bonds between the polymer and the nanoparticles increases the adhesion force, making it harder for the water molecules to diffuse through the film [46]. Similar results were observed in previous studies, where the WVP decreased in the gelatin/k-carrageenan film with the incorporation of SiO_2 nanoparticles [34], as well as in the SRIC films with the incorporation of ZnO nanoparticles [1].

3.6. Wettability

The wettability of the films presented in the form of critical surface tension (CST). The incorporation of nanoparticles did not significantly affect the CST of the films (Table 2). Moreover, from the data presented in Table 2, it can be seen that the standard deviation of the IC and IC/SiO_2 films was larger than that of other films, which may be affected by outliers in the data collected. The adhesive forces between the liquid and the solid surface favor to spread of the liquid drop on a solid surface, contrary, the cohesive forces within the liquid counteract the spreading. The liquid drop spreads with the contact angle of 0° and undergoes complete wetting when a solid surface has surface energy higher than the surface tension of the liquid [37].

The surface energy or the critical surface tension of the films in this study ranges from 18.603-22.137 mN/m, which still much lower than the surface tension of water (72.8 mN/m), thus resulting in a large water contact angle (>90°), and the film surfaces are said to be hydrophobic [37, 47]. The CST of all the film types did not differ significantly. However, the slight increase in the CST of the films with nanoparticles might be due to the differences in the surface structure of the films, as seen in the AFM test results, where the IC film had a wavier and more uneven surface than the films with nanoparticles. The roughness of a

Table 1. Thickness, Tensile Strength (TS), Elongation at Break (EAB), and Water Vapor Permeability (WVP) of the bio-nanocomposite films*.

Film Type	Thickness (mm)	TS (MPa)	EAB (%)	WVP (10^{-6} g/h.m.Pa)
IC	$0.067^{a} \pm 0.002$	$18.36^{a} \pm 0.90$	$9.86^{a} \pm 2.15$	$1.059^{b} \pm 0.036$
IC/SiO_2	$0.071^{b} \pm 0.001$	$19.37^{ab} \pm 0.52$	$10.92^{a} \pm 1.91$	$1.035^{b} \pm 0.074$
IC/ZnO	$0.070^{b} \pm 0.001$	$19.42^{ab} \pm 2.32$	$9.17^{a} \pm 0.66$	$1.031^{b} \pm 0.047$
IC/SiO_2–ZnO 1:1	$0.066^{a} \pm 0.001$	$15.82^{a} \pm 1.07$	$8.97^{a} \pm 1.56$	$1.011^{b} \pm 0.032$
IC/SiO_2–ZnO 1:2	$0.064^{a} \pm 0.003$	$17.92^{a} \pm 5.34$	$8.54^{a} \pm 4.22$	$0.996^{ab} \pm 0.041$
IC/SiO_2–ZnO 1:3	$0.067^{a} \pm 0.001$	$24.59^{b} \pm 4.75$	$9.00^{a} \pm 3.47$	$0.918^{a} \pm 0.048$

*Values are presented as mean ± SD (n = 3). Different letters in the same column indicate significantly different ($p < 0.05$).

Table 2. Critical surface tension (CST) of the bio-nanocomposite films*.

Film Type	CST (mN/m)
IC	$18.603^{a} \pm 2.928$
IC/SiO_2	$19.564^{a} \pm 2.425$
IC/ZnO	$19.580^{a} \pm 0.605$
IC/SiO_2–ZnO 1:1	$22.137^{a} \pm 2.047$
IC/SiO_2–ZnO 1:2	$21.496^{a} \pm 1.758$
IC/SiO_2–ZnO 1:3	$21.430^{a} \pm 0.589$

*Values are presented as mean ± SD (n = 3). Different letters in the same column indicate significantly different ($p < 0.05$).

solid surface creates empty spaces and air pockets that hold and prevent the liquid from wetting the solid surface, and then resulting in a greater contact angle [48].

3.7. Optical properties

Figure 3 presents the transmittance spectrum of Ultraviolet (UV) (200–400 nm) to visible light (400–700 nm). The UV light transmittance through the film decreased with the addition of SiO_2 and ZnO nanoparticles. The film with the highest UV transmittance was the IC film, followed by the IC/ZnO film, IC/SiO_2 film, IC/SiO_2–ZnO 1:1 film, IC/SiO_2–ZnO film 1:3, and IC/SiO_2–ZnO 1:2 film. This indicates that the SiO_2 and ZnO nanoparticles increase the absorption of UV light by the film so that it can promote a protective effect against UV (UV-screening), thereby reducing the interaction of UV with food and thus preventing oxidation.

The UV transmittance decreased as the concentration of ZnO nanoparticles was increased. This is due to the ability of ZnO to absorb UV light, thereby reducing the transmission of UV light that passes through the film. ZnO is a semiconductor material with bandgap energy (Eg) of ~3.37 eV, so it can absorb UV light with photon energy ($h\nu$) equal to or greater than the excitation energy/bandgap energy (wavelength equal to or less than 376 nm) [49, 50].

Percent transmittance at a wavelength of visible light (400–700 nm) shows the amount of visible light that can be transmitted through the film. Hence, the greater the transmission, the better the film transparency [1]. The IC/ZnO and the IC/SiO_2 films were the films with the highest transparency. Although the transparency decreased when the two nanoparticles were combined, generally the addition of SiO_2 and ZnO nanoparticles did not interfere with the transparency of the film, indicating that the incorporated nanoparticles had good compatibility with the film matrix, thus supporting the transmission of visible light through the film [1].

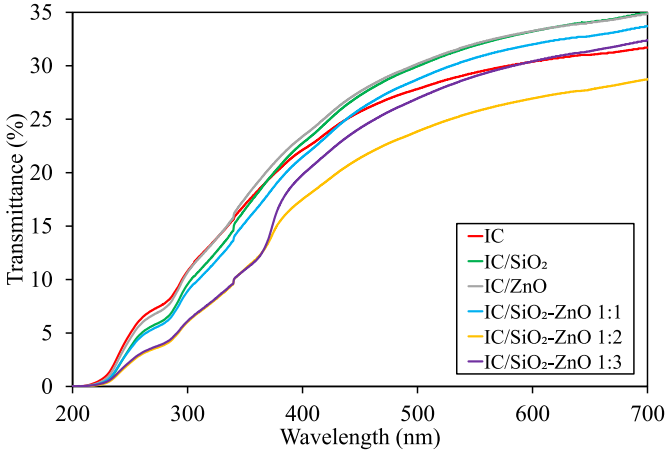

Figure 3. UV-vis transmittance spectrum of the bio-nanocomposite films.

3.8. Antimicrobial activity

The antimicrobial activity of the films in this study is the inhibitory activity against the growth of pathogenic microbes *Staphylococcus aureus* (gram-positive bacteria) and *Escherichia coli* (gram-negative bacteria), presented in the form of inhibitory zone diameter (mm). The greater the inhibition zone formed, the better the ability of the film to inhibit microbial growth. As presented in Table 3, the IC film did not exhibit antimicrobial activity, while the films with the incorporation of SiO_2 and ZnO nanoparticles separately only exhibited inhibitory activity against *E. coli*. The films with a mixture of SiO_2–ZnO exhibited antimicrobial activity against both types of bacteria, indicating the synergy effect of both nanoparticles in inhibiting microbial growth.

Generally, the inhibitory activity in this study was found to be greater against *E. coli* than *S. aureus*. This indicates that *E. coli* has greater susceptibility to SiO_2 and ZnO nanoparticles than *S. aureus*. The cationic metal ions from the nanoparticles have a higher affinity to gram-negative bacteria than to gram-positive bacteria, promoting enhanced antimicrobial activity against gram-negative bacteria [31]. Also, the difference in the intracellular antioxidant content of these two bacteria, such as the carotenoid pigments in the interior of *S. aureus* promotes higher oxidant resistance, and also the presence of strong detoxification agents such as antioxidant enzymes (catalase) [18]. Other studies have also reported similar results on the antimicrobial activity of the nanoparticle-loaded films [5, 31, 51].

The mechanism of nanoparticles against microorganisms is associated with the release of antimicrobial ions from the nanoparticles such as Zn^{2+} into the medium containing the microorganisms [18]. Electrostatic interactions between the positive charge of metal ions and the negative charge of bacterial membranes and biomolecules (DNA and protein) cause structural damage and consequently, the death of bacteria [31]. The absence of antimicrobial activity in the IC/SiO_2 and IC/ZnO films against *S. aureus* might also due to the concentration of nanoparticles which was too low to promote any antimicrobial effect. Furthermore, the release of ions from the nanoparticles depends on their concentration and time, so if the ion concentration is too low it may encourage relatively high tolerance to microorganisms, and even increase bacterial growth [18].

Particle size also affects antimicrobial activity. Nanoparticles with a size less than 100 nm are more abrasive thus contributing to greater mechanical damage to bacterial cell membranes and increasing their antimicrobial effect on films [52]. The smaller the size of the nanoparticles will increase the effectiveness of the antimicrobial because of their large surface area, thus increasing the contact area with microbes, and the smaller the size of the nanoparticles the easier their penetration into the cell walls [18, 53]. From the particle size distribution analyses carried out in the previous study [29], the SiO_2 NPs suspension and ZnO NPs suspension had a larger particle size than the SiO_2–ZnO NPs combination suspension. So that in this study, films with the incorporation of SiO_2–ZnO nanoparticles showed greater antimicrobial activity.

3.9. Water-solubility

The percent of film solubility increased with the addition of the nanoparticles. The highest solubility was observed in the IC/SiO_2 film (85.88%), followed by IC/SiO_2–ZnO 1:2 film (74.85%), IC/ZnO film (74.69%), IC/SiO_2–ZnO 1:3 film (73.47%), IC/SiO_2–ZnO 1:1 film (73.20%), and the lowest was in the IC film without nanoparticles (66.48%). The increase of film solubility in water with the presence of nanoparticles was also reported in other studies [20, 45, 54]. The high water-solubility of the film is due to the hydrophilic nature of the iota carrageenan provided by the presence of sulfate groups and hydroxyl groups [55]. This increase in solubility may be due to the interaction of the nanoparticles with the carrageenan polymers in the film matrix, which may affect the carrageenan molecular forces by reducing the cohesion force, or may affect the equilibrium of the cations in aqueous

Table 3. Antimicrobial activity of the bio-nanocomposite films*.

Film Type	Inhibition Zone (mm)	
	E. coli	*S. aureus*
IC	$0.000^{a} \pm 0.000$	$0.000^{a} \pm 0.000$
IC/SiO_2	$15.283^{b} \pm 1.553$	$0.000^{a} \pm 0.000$
IC/ZnO	$21.224^{c} \pm 2.518$	$0.000^{a} \pm 0.000$
IC/SiO_2–ZnO 1:1	$24.814^{c} \pm 0.446$	$13.450^{b} \pm 0.229$
IC/SiO_2–ZnO 1:2	$23.910^{c} \pm 2.082$	$16.217^{c} \pm 0.597$
IC/SiO_2–ZnO 1:3	$21.508^{c} \pm 4.477$	$15.683^{c} \pm 0.562$

*Values are presented as mean ± SD (n = 3). Different letters in the same column indicate significantly different ($p < 0.05$).

solutions, considering that the solubility of carrageenan in water does not only depend on the number of sulfate groups but also the cations [56].

3.10. Degradability

The degradation rate of the films in the soil is shown in the form of weight (%) over 4 weeks (Figure 4). The weight reduction indicates the degradability of the film. After the first week, the weight of all film types was increased due to the absorption of water by the hydrophilic SRIC films from the moist soil. The films started to degrade in the following week, and by the fourth week, almost all the films had degraded completely. In general, it can be seen that the IC/ZnO, IC/SiO_2, and IC/SiO_2–ZnO 1:2 films exhibited better degradability than the IC film, while the IC/SiO_2–ZnO 1:1 and the IC/SiO_2–ZnO 1:3 films tended to degrade more slowly than the IC film. The films were degraded by the enzymatic reactions of living organisms (bacteria, yeast, and mold). With the presence of particular enzymes, the polymer chain is broken into small fragments that the microorganisms used as energy sources [57, 58]. This result indicates that the incorporation of SiO_2 and ZnO nanoparticles separately did not impede the bio-degradation process of the film, but their mixtures could slow down the degradation process. Some researchers suggest that nanoparticles provide a catalyst effect on the process of biodegradation or hydrolysis degradation, while others suggest that nanoparticles inhibit the degradation of polymers because their large aspect ratios and their dispersion in the film matrix provides more tortuous pathways which will impede and prevent the penetration and diffusion of microorganisms into the film matrix [12]. In this study, the films with SiO_2–ZnO nanoparticles showed an antimicrobial effect, thus preventing the microorganisms from degrading the films.

3.11. Determination of the best film type

The best film type was determined by a compensatory model using a non-dimensional scaling model [59]. The variables used to determine the best film type were the mechanical properties (TS and EAB), WVP, optical properties (transparency at λ = 660 nm, and UV-screening at λ = 280 nm), and antimicrobial activity. This method was implemented firstly by determining the best and worst values of the analysis results for each variable. Variable Weight (VW) then was assigned to each variable, from 0-1 based on its value to the film quality. In this study, the Variable Weight (VW) for all the variables used was 1, which means that they all had equal value to the film quality. The next step was to determine the Normalization Weight (NW) for each variable using Eq. (5):

$$NW = \frac{VW}{\sum VW} \tag{5}$$

and to calculate the Non-Dimensional Value (NV) using Eq. (6):

$$NV = \frac{value - worst\ value}{best\ value - worst\ value} \tag{6}$$

Then the scores (NW x NV) were calculated for all the variables in each film type. The film with the highest total score was determined to be the best film type. In this study, after all the calculations were completed, the IC/SiO_2–ZnO 1:3 film appeared to be the best film type as it got the highest total score (0.794) compared to all the other types of film, followed by IC/SiO_2–ZnO 1:2 film (0.521), IC/SiO_2–ZnO 1:1 film (0.517), IC/SiO_2 film (0.511), IC/ZnO film (0.407), and IC film which had the lowest total score (0.194).

3.12. Thermal stability

Figure 5 represents the thermal stability of the IC film and the IC/SiO_2–ZnO 1:3 film, which was determined to the best film type. Two stages of thermal decomposition were found to occur. The first was the evaporation process of the water loaded in the film, which began in the early heating process [60]. The second stage started to occur at around 235 °C for the IC film and 260 °C for the IC/SiO_2–ZnO 1:3 film. This was the decomposition of carrageenan as the main film matrix and the evaporation of glycerol [61]. It can be seen that there was a difference in decomposition temperature between the two types of film, which indicates that the film with nanoparticles (IC/SiO_2–ZnO 1:3) had better thermal stability than the film without nanoparticles (IC). However, at 500 °C the percent residual was less for the IC/SiO_2–ZnO 1:3 film (26.30%) than for the IC film (36.23%). This is related to the first stage of decomposition in which the IC/SiO_2–ZnO 1:3 film had greater weight loss than the IC film, indicating that the presence of nanoparticles reduced the formation of hydrogen bonds between water and the film matrix, thus increasing the amount of water being evaporated [44].

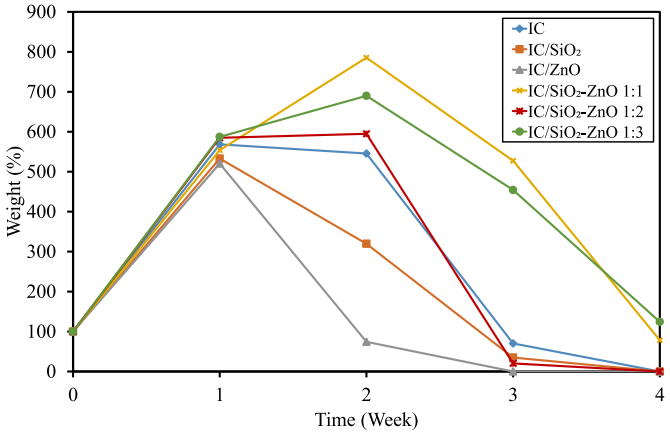

Figure 4. Degradability of the bio-nanocomposite films.

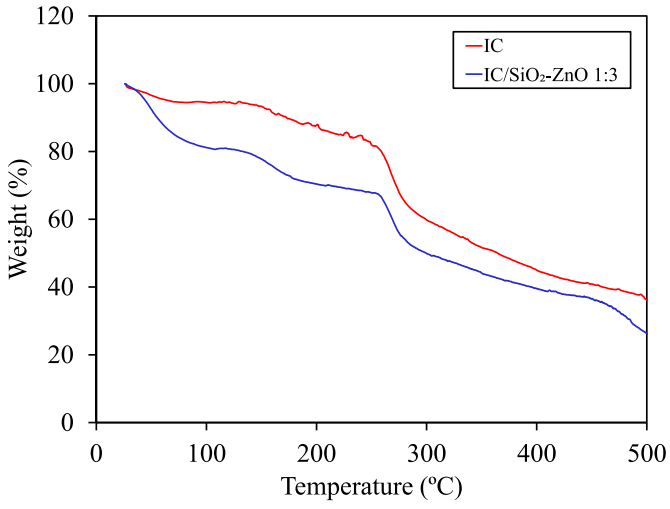

Figure 5. Thermal stability of the bio-nanocomposite films.

4. Conclusion

The incorporation of SiO_2 and ZnO nanoparticles into SRIC-based film has reinforced the films multifunctional properties with enhanced water vapor barrier properties, UV-screening, and antimicrobial activity. Also, to some extent, it did not cause loss of other useful properties of the film, such as transparency, water-solubility, degradability, and thermal stability. Moreover, it was found that reinforcement with SiO_2–ZnO improved the tensile strength of the film. While the elongation at break and wettability did not differ significantly between all of the film types. The improvement in film properties is considered influenced by a well-dispersed fillers suspension which was evenly distributed within the matrix, creating strong interaction between nanoparticle fillers and the film matrix. The surface morphology of the film also seemed to be affected by the presence of the nanoparticles. It is concluded that the best performance of the prepared active packaging films is the IC/SiO_2–ZnO 1:3 film. Thus, this formulation of films provides a potential opportunity to serve as an active food packaging film and as an excellent alternative to petrochemical-based food packaging.

Declarations

Author contribution statement

Danar Praseptiangga: Conceived and designed the experiments; Performed the experiments; Analyzed and interpreted the data; Contributed reagents, materials, analysis tools or data; Wrote the paper.

Nuha Mufida: Performed the experiments; Analyzed and interpreted the data; Wrote the paper.

Camellia Panatarani: Analyzed and interpreted the data; Contributed reagents, materials, analysis tools or data; Wrote the paper.

I. Made Joni: Conceived and designed the experiments; Analyzed and interpreted the data; Contributed reagents, materials, analysis tools or data; Wrote the paper.

Funding statement

This work was supported by Hibah Riset Internal Unpad (1427/UN6.3.1/LT/2020).

Data availability statement

Data included in article/supplementary material/referenced in article.

Declaration of interests statement

The authors declare no conflict of interest.

Additional information

No additional information is available for this paper.

Acknowledgements

We are grateful to Dr. Risa Suryana (Universitas Sebelas Maret) for his help in observing the surface morphology of the films using Atomic Force Microscopy (AFM).

References

[1] A.R. Khoirunnisa, I.M. Joni, C. Panatarani, E. Rochima, D. Praseptiangga, UV-screening, transparency and water barrier properties of semi refined iota carrageenan packaging film incorporated with ZnO nanoparticles, in: AIP Conf. Proc., 2018, pp. 1–8.

[2] N.P. Risyon, S.H. Othman, R.K. Basha, R.A. Talib, Characterization of polylactic acid/halloysite nanotubes bionanocomposite films for food packaging, Food Packag. Shelf Life. 23 (2020) 100450.

[3] G. El Fawal, H. Hong, X. Song, J. Wu, M. Sun, C. He, X. Mo, Y. Jiang, H. Wang, Fabrication of antimicrobial films based on hydroxyethylcellulose and ZnO for food packaging application, Food Packag. Shelf Life. 23 (2020) 100462.

[4] H.P.S. Abdul Khalil, C.K. Saurabh, Y.Y. Tye, T.K. Lai, A.M. Easa, E. Rosamah, M.R.N. Fazita, M.I. Syakir, A.S. Adnan, H.M. Fizree, N.A.S. Aprilia, A. Banerjee, Seaweed based sustainable films and composites for food and pharmaceutical applications: a review, Renew. Sustain. Energy Rev. 77 (2017) 353–362.

[5] N.A. Al-Tayyar, A.M. Youssef, R.R. Al-Hindi, Antimicrobial packaging efficiency of ZnO-SiO2 nanocomposites infused into PVA/CS film for enhancing the shelf life of food products, Food Packag. Shelf Life. 25 (2020) 100523.

[6] S. Kumar, J.C. Boro, D. Ray, A. Mukherjee, J. Dutta, Bionanocomposite films of agar incorporated with ZnO nanoparticles as an active packaging material for shelf life extension of green grape, Heliyon 5 (2019), e01867.

[7] D. Praseptiangga, S. Giovani, D.R.A. Muhammad, G.J. Manuhara, Development of edible film from semi refined iota carrageenan for sustainable food packaging, ARPN J. Eng. Appl. Sci. 13 (2018) 8907–8918.

[8] D. Praseptiangga, Development of seaweed-based biopolymers for edible films and lectins, in: IOP Conf. Ser. Mater. Sci. Eng., 2017.

[9] D. Praseptiangga, S. Giovani, G.J. Manuhara, D.R.A. Muhammad, Formulation and characterization of novel composite semi-refined iota carrageenan-based edible film incorporating palmitic acid, in: AIP Conf. Proc., 2017.

[10] R. Thakur, B. Saberi, P. Pristijono, J. Golding, C. Stathopoulos, C. Scarlett, M. Bowyer, Q. Vuong, Characterization of rice starch-ι-carrageenan biodegradable edible film. Effect of stearic acid on the film properties, Int. J. Biol. Macromol. 93 (2016) 952–960.

[11] N.A. Al-Tayyar, A.M. Youssef, R. Al-hindi, Antimicrobial food packaging based on sustainable Bio-based materials for reducing foodborne Pathogens: a review, Food Chem. 310 (2020) 125915.

[12] M. Šupová, G.S. Martynková, K. Barabaszová, Effect of nanofillers dispersion in polymer matrices: a review, Sci. Adv. Mater. 3 (2011) 1–25.

[13] A.M. Youssef, S.M. El-Sayed, Bionanocomposites materials for food packaging applications: concepts and future outlook, Carbohydr. Polym. 193 (2018) 19–27.

[14] S.M. El-Sayed, H.S. El-Sayed, O.A. Ibrahim, A.M. Youssef, Rational design of chitosan/guar gum/zinc oxide bionanocomposites based on Roselle calyx extract for Ras cheese coating, Carbohydr. Polym. 239 (2020) 116234.

[15] F. Bi, X. Zhang, J. Liu, H. Yong, L. Gao, J. Liu, Development of antioxidant and antimicrobial packaging films based on chitosan, D-α-tocopheryl polyethylene glycol 1000 succinate and silicon dioxide nanoparticles, Food Packag. Shelf Life. 24 (2020) 100503.

[16] N. Bumbudsanpharoke, J. Choi, H.J. Park, S. Ko, Zinc migration and its effect on the functionality of a low density polyethylene-ZnO nanocomposite film, Food Packag. Shelf Life. 20 (2019).

[17] A.M. Youssef, F.M. Assem, H.S. El-Sayed, S.M. El-Sayed, M. Elaaser, M.H. Abd El-Salam, Synthesis and evaluation of eco-friendly carboxymethyl cellulose/polyvinyl alcohol/CuO bionanocomposites and their use in coating processed cheese, RSC Adv. 10 (2020) 37857–37870.

[18] P.J.P. Espitia, N.F.F. de Soares, J.S.R. dos Coimbra, N.J. de Andrade, R.S. Cruz, E.A.A. Medeiros, Zinc oxide nanoparticles: synthesis, antimicrobial activity and food packaging applications, Food Bioprocess Technol. 5 (2012) 1447–1464.

[19] S. Shankar, J.W. Rhim, Effect of types of zinc oxide nanoparticles on structural, mechanical and antibacterial properties of poly(lactide)/poly(butylene adipate-co-terephthalate) composite films, Food Packag. Shelf Life. 21 (2019) 100327.

[20] A.E. Saputri, D. Praseptiangga, E. Rochima, C. Panatarani, I.M. Joni, Mechanical and solubility properties of bio-nanocomposite film of semi refined kappa carrageenan/ZnO nanoparticles, in: AIP Conf. Proc., 2018.

[21] A.I. Aji, D. Praseptiangga, E. Rochima, I.M. Joni, C. Panatarani, Optical transparency and mechanical properties of semi-refined iota carrageenan film reinforced with SiO2 as food packaging material, in: AIP Conf. Proc., 2018, pp. 1–7.

[22] R. Venkatesan, N. Rajeswari, T.T. Thiyagu, Preparation, characterization and mechanical properties of K-carrageenan/SiO2 nanocomposite films for antimicrobial food packaging, Bull. Mater. Sci. 40 (2017) 609–614.

[23] L.R. Rane, N.R. Savadekar, P.G. Kadam, S.T. Mhaske, Preparation and characterization of K-carrageenan/nanosilica biocomposite film, J. Mater. 2014 (2014) 1–8.

[24] I.M. Joni, M. Vanitha, C. Panatarani, F. Faizal, Dispersion of amorphous silica nanoparticles via beads milling process and their particle size analysis, hydrophobicity and anti-bacterial activity, Adv. Powder Technol. 31 (2020) 370–380.

[25] I.M. Joni, T. Ogi, A. Purwanto, K. Okuyama, T. Saitoh, K. Takeuchi, Decolorization of beads-milled TiO2 nanoparticles suspension in an organic solvent, Adv. Powder Technol. 23 (2012) 55–63.

[26] I.M. Joni, C. Panatarani, D.W. Maulana, Dispersion of fine phosphor particles by newly developed beads mill, in: I.M. Joni, C. Panatarani (Eds.), AIP Conf. Proc., American Institute of Physics, Melville, NY, 2016, pp. 500191–500196.

[27] I.M. Joni, C. Panatarani, D. Hidayat, Setianto, B.M. Wibawa, A. Rianto, H. Thamrin, Synthesis and dispersion of nanoparticles, and Indonesian graphite processing, in: AIP Conf. Proc. 1554, 2013, pp. 20–26.

[28] T. Ogi, R. Zulhijah, T. Iwaki, K. Okuyama, Recent progress in nanoparticle dispersion using bead mill, KONA Powder Part. J. 2017 (2017) 3–23.

[29] C. Panatarani, N. Mufida, D. Widyaastuti, D. Praseptiangga, I.M. Joni, Dispersion of SiO2 and ZnO nanoparticles by bead milling in the preparation of carrageenan bio-nanocomposite film, in: AIP Conf. Proc, American Institute of Physics, 2020, p. 100002.

[30] D. Praseptiangga, H.L. Zahara, P.I. Widjanarko, I.M. Joni, C. Panatarani, Preparation and FTIR spectroscopic studies of SiO2-ZnO nanoparticles suspension for the development of carrageenan-based bio-nanocomposite film, in: AIP Conf. Proc., 2020, p. 100005.
[31] A.A. Oun, J.W. Rhim, Carrageenan-based hydrogels and films: effect of ZnO and CuO nanoparticles on the physical, mechanical, and antimicrobial properties, Food Hydrocolloids 67 (2017) 45–53.
[32] A. Farhan, N.M. Hani, Characterization of edible packaging films based on semi-refined kappa-carrageenan plasticized with glycerol and sorbitol, Food Hydrocolloids 64 (2017) 48–58.
[33] M. Beigomi, M. Mohsenzadeh, A. Salari, Characterization of a novel biodegradable edible film obtained from Dracocephalum moldavica seed mucilage, Int. J. Biol. Macromol. 108 (2018) 874–883.
[34] R.H. Tabatabaei, S.M. Jafari, H. Mirzaei, A. Mohammadi Nafchi, D. Dehnad, Preparation and characterization of nano-SiO2 reinforced gelatin-k-carrageenan biocomposites, Int. J. Biol. Macromol. 111 (2018) 1091–1099.
[35] ASTM, Standard Test Method for Tensile Properties of Thin Plastic Sheeting 1, 2002, pp. 1–9, 14.
[36] J. Yu, J. Yang, B. Liu, X. Ma, Preparation and characterization of glycerol plasticized-pea starch/ZnO-carboxymethylcellulose sodium nanocomposites, Bioresour. Technol. 100 (2009) 2832–2841.
[37] G. Lamour, A. Hamraoui, A. Buvailo, Y. Xing, S. Keuleyan, V. Prakash, A. Eftekhari-Bafrooei, E. Borguet, Contact angle measurements using a simplified experimental setup, J. Chem. Educ. 87 (2010) 1403–1407.
[38] P. Kanmani, J.W. Rhim, Properties and characterization of bionanocomposite films prepared with various biopolymers and ZnO nanoparticles, Carbohydr. Polym. 106 (2014) 190–199.
[39] CLSI, M2-A9, Performance standards for antimicrobial disk susceptibility tests; approved standard—ninth edition, Clin. Lab. Stand. Inst. 26 (2006) 1–37.
[40] P.K. Swain, M. Das, P.L. Nayak, Biodegradation studies of chitosan-polycaprolactone (PCL) nanocomposite in soil burial test, middle-east, J. Sci. Res. 23 (2015) 253–258.
[41] J.W. Rhim, L.F. Wang, Preparation and characterization of carrageenan-based nanocomposite films reinforced with clay mineral and silver nanoparticles, Appl. Clay Sci. (2014) 97–98, 174–181.
[42] R.N. Jagtap, A.H. Ambre, Overview literature on atomic force microscopy (AFM): basics and its important applications for polymer characterization, Indian J. Eng. Mater. Sci. 13 (2006) 368–384.
[43] R.L. Pecsok, L.D. Shields, T. Cairns, I.G. McWilliam, Modern Methods of Chemical Analysis, second ed., John Wiley & Sons, Inc., New York, 1976.
[44] S. Ghazihoseini, N. Alipoormazandarani, A.M. Nafchi, The effects of nano-SiO2 on mechanical, barrier, and moisture sorption isotherm models of novel soluble soybean polysaccharide films, Int. J. Food Eng. 11 (2015) 833–840.
[45] A. Babaei-Ghazvini, I. Shahabi-Ghahfarrokhi, V. Goudarzi, Preparation of UV-protective starch/kefiran/ZnO nanocomposite as a packaging film: Characterization, Food Packag. Shelf Life. 16 (2018) 103–111.
[46] I. Shahabi-Ghahfarrokhi, F. Khodaiyan, M. Mousavi, H. Yousefi, Preparation of UV-protective kefiran/nano-ZnO nanocomposites: physical and mechanical properties, Int. J. Biol. Macromol. 72 (2015) 41–46.
[47] T. Zhao, L. Jiang, Contact angle measurement of natural materials, Colloids Surf. B Biointerfaces 161 (2018) 324–330.
[48] W.A. Zisman, Relation of the equilibrium contact angle to liquid and solid constitution, in: Adv. Chem. Ser., American Chemical Society, Washington DC, 1964, pp. 1–51.
[49] C.B. Ong, L.Y. Ng, A.W. Mohammad, A review of ZnO nanoparticles as solar photocatalysts: synthesis, mechanisms and applications, Renew. Sustain. Energy Rev. 81 (2018) 536–551.
[50] M.S. Ghamsari, S. Alamdari, W. Han, H. Park, Impact of nanostructured thin ZnO film in ultraviolet protection, Int. J. Nanomed. 12 (2017) 207–216.
[51] M. Azizi-Lalabadi, M. Alizadeh-Sani, B. Divband, A. Ehsani, D.J. McClements, Nanocomposite films consisting of functional nanoparticles (TiO2 and ZnO) embedded in 4A-Zeolite and mixed polymer matrices (gelatin and polyvinyl alcohol), Food Res. Int. 137 (2020) 109716.
[52] A. Kołodziejczak-Radzimska, T. Jesionowski, Zinc oxide — from synthesis to application: a review, Materials 7 (2014) 2833–2881.
[53] A.M. Nafchi, A.K. Alias, S. Mahmud, M. Robal, Antimicrobial, rheological, and physicochemical properties of sago starch films filled with nanorod-rich zinc oxide, J. Food Eng. 113 (2012) 511–519.
[54] M.V. Aristizabal-Gil, S. Santiago-Toro, L.T. Sanchez, M.I. Pinzon, J.A. Gutierrez, C.C. Villa, ZnO and ZnO/CaO nanoparticles in alginate films. Synthesis, mechanical characterization, barrier properties and release kinetics, LWT (Lebensm.-Wiss. & Technol.) 112 (2019) 108217.
[55] C.P. Kelco, GENU ® Carrageenan Book, 2001, pp. 4–23. https://foodsci.rutgers.edu/carbohydrates/Carrageenan Book.pdf.
[56] V.L. Campo, D.F. Kawano, D.B. da Silva, I. Carvalho, Carrageenans, Biological properties, chemical modifications and structural analysis - a review, Carbohydr. Polym. 77 (2009) 167–180.
[57] A.N. Malathi, K.S. Santhosh, N. Udaykumar, Recent trends of biodegradable polymer: biodegradable films for food packaging and application of nanotechnology in biodegradable food packaging, Curr. Trends Technol. Sci. 3 (2014) 73–79.
[58] H. Wang, D. Wei, A. Zheng, H. Xiao, Soil burial biodegradation of antimicrobial biodegradable PBAT films, Polym. Degrad. Stabil. 116 (2015) 14–22.
[59] W.G. Sullivan, E.M. Wicks, C.P. Koelling, Engineering Economy, sixteenth ed., Pearson Education Ltd., London, 2015.
[60] S. Shankar, J.W. Rhim, Preparation and characterization of agar/lignin/silver nanoparticles composite films with ultraviolet light barrier and antibacterial properties, Food Hydrocolloids 71 (2017) 76–84.
[61] S. Roy, J.W. Rhim, Carrageenan-based antimicrobial bionanocomposite films incorporated with ZnO nanoparticles stabilized by melanin, Food Hydrocolloids 90 (2019) 500–507.